
Article:
Espejo, C, Wang, C orcid.org/0000-0002-4301-3974, Thiébaut, B et al. (3 more authors) (2020) The role of MoDTC tribochemistry in engine tribology performance. A Raman microscopy investigation. Tribology International, 150. 106366. ISSN 0301-679X

https://doi.org/10.1016/j.triboint.2020.106366

The role of MoDTC tribochemistry in Engine Tribology Performance. A Raman microscopy investigation.

Cayetano Espejo[1], Chun Wang[1], Benoît Thiébaut[2], Catherine Charrin[2], Anne Neville[1], Ardian Morina[1]

Abstract

In order to tackle the new challenges towards the reduction of carbon emissions in transport industry, the present work aims to understand the effect of the friction modifier (FM) molybdenum dithiocarbamate (MoDTC) on the performance of an automobile engine. A petrol engine has undergone motored test trials, measuring the friction torque reduction when the FM additive is blended into a fully formulated SAE 5W30 oil. Moreover, the engine has been dismantled after the test, investigating the tribochemistry of MoDTC at different key engine components undergoing boundary lubrication, using Raman microscopy. This work demonstrates that materials and contact pressure play a crucial role in MoDTC tribochemistry to form a low friction tribofilm, contributing to global engine friction reduction.

[1] Institute of Functional Surfaces, School of Mechanical Engineering, University of Leeds, LS2 9JT, Leeds, United Kingdom

[2] TOTAL, Centre de Recherche de Solaize, Chemin du Canal BP 22-69360 Solaize, France

[*]Corresponding author: c.espejoconesa@leeds.ac.uk

1. Introduction

One of the main targets in automobile oil development is to increase fuel efficiency by means of reducing friction losses. To achieve this goal the general trend is designing oils with lower viscosity, as most of the frictional losses are produced in components in hydrodynamic regime contact. This trend is supported by the elaboration of new standards including lower viscosity oils that satisfy the needs from Original Equipment Manufacturers (OEMs) [1]. However, the use of these types of oils will exacerbate the transition of several systems into boundary lubrication (BL), delivering not only higher friction but also promoting excessive wear, compromising the engine durability. In order to reduce the impact of this shift towards BL, OEMs are currently designing engines to be run with low viscosity oils, tailoring geometrical dimensions and using wear-resistant coatings, such as Physical Vapour Deposition (PVD) produced CrN or Diamond-Like-Carbon coatings (DLC).

In this scenario it is crucial to find a good compromise between the low friction performance provided by low viscosity oils and the low wear performance provided by shifting engine tribosystems towards the hydrodynamic regime. This is especially challenging, as regardless of the engine design, different systems within the engine will run under different lubrication regimes.

A good strategy to overcome these difficulties is to lower the viscosity of the oil, reducing the friction in tribological systems under the hydrodynamic regime, while using specific additives to control the wear and friction in the engine systems working in boundary lubrication. These additives are called Friction Modifiers (FM), and nowadays different chemistries are involved depending on the engine target working conditions. Among these additives, molybdenum dithiocarbamate (MoDTC) is demonstrated as a very efficient additive [2] present in many commercially available Fully Formulated (FF) oils. This additive, under certain tribological conditions leads to MoS_2 formation on the surface. MoS_2 is an excellent solid lubricant, which reduces friction due to its layered crystalline structure with weak bonds between lamellar sheets [3], that are easily broken under shear stress, delivering low friction. In this context, it is crucial to understand the interactions between the different additives of a FF oil, and between the additives and the surfaces in tribological contact. Special consideration has to be adopted to the engine component materials and coatings, as both positive and negative interactions may occur between the surfaces and the oil additives [4-8].

To assess the performance of engine oils from the tribological point of view, several rigs are currently used. Standard tribometers such as unidirectional sliding pin-on-disk [9], reciprocating pin-on-plate [10], mini-traction-machine [11], among others, are useful tools to assess the tribochemistry of the additives. These rigs can emulate to some extent the tribological contact inside and engine, by means of controlling variables such as temperature, speed or contact pressure. However, true conditions in car engines differ from those achievable with standard tribometers. Several materials, geometries, temperature profiles, contact pressures, rolling/sliding ratios and environments are involved in different parts of the engine, making even more challenging to select the proper rig to evaluate the oil performance [5].

Fired engine tests are the closest method to determine the efficiency of the oil used, as a standardised method simulating driving conditions with all operational fluids resembles the conventional use of an engine. However these tests require accurate instrumentation to control critical parameters, such as torque, speed, exhaust pressure, temperature in different places, gas analysis, etc [12].

Another approach involves the use of a motored test, which complies with the geometry, materials and, to a lesser extent, the mechanics of the contact. It has been proven in literature that similar friction data is acquired when comparing motored and fired engine tests [13]. An advantage of motored tests is that engine friction losses can be isolated from other non-tribological related phenomena and resolved into different operating systems, targeting the systems that account for most of the losses for every lubricant formulation [14]. The main drawback of this strategy is neglecting the effect of the combustion gases, the high cylinder pressure, and unburned fuel in the engine oil performance [15, 16], which especially affects the sludge production and the durability of the oil [17].

As mentioned in the previous paragraphs, MoDTC functions in reducing friction by means of tribochemistry reactions. Shear, temperature and surface chemistry promote the formation of MoS_2 from MoDTC, a well-known solid lubricant. To detect the

formation of this compound on the surfaces in contact, several techniques may be used, being Raman microscopy a powerful tool. This technique presents numerous advantages in comparison to EDX, XPS or SIMS, allowing for example, accurate distinction between MoS_2 and other molybdenum species in a non-vacuum environment [18] and a spatial distribution semi-quantification that can be linked to the friction performance [19].

In this work, after confirming that friction reduction is achieved in a full engine motored test by the addition of MoDTC additive, Raman microscopy is used in a set of engine parts obtained afterwards. The areas of interest are then located to identify the formation of the friction-reducing tribofilm, and to find and explain the friction reduction in the engine when molybdenum-containing oils are used. Methodologies and results are evaluated, comparing the output with literature on bench tribotests using similar conditions and material tribopairs, opening new strategies for molybdenum tribochemistry prediction in real engine systems using fully formulated oils.

2. Experimental

A motored test was executed using a SAE 5W30 ACEA A5/B5 fully formulated oil, elaborated from a group III basestock, firstly with no MoDTC, secondly with added MoDTC (1000 ppm Mo).

The tested unit was a Nissan HR12DDR engine, consisting of a 1.2L straight three cylinder gasoline engine with direct acting DOHC system [20]. The main features of this engine are listed in Table 1.

Table 1. Main features of the engine used in this study.

Configuration	Straight-3
Bore x Stroke	78.0 x 83.6
Displacement	1198 cc
Compression Ratio	13:1
Max Power	72 kW @ 5200 rpm
Max Torque	142 Nm @ 4400 rpm
Valve train system	Direct acting DOHC
Aspiration	Supercharger
Fuel supply	Direct injection

To carry out the motored test, a Friction Torque Test (FTT) has been chosen, in order to ensure representative and high precision measurements.

The testing conditions are similar to the FTT methodology considered for the new JASO M365 standard [21].

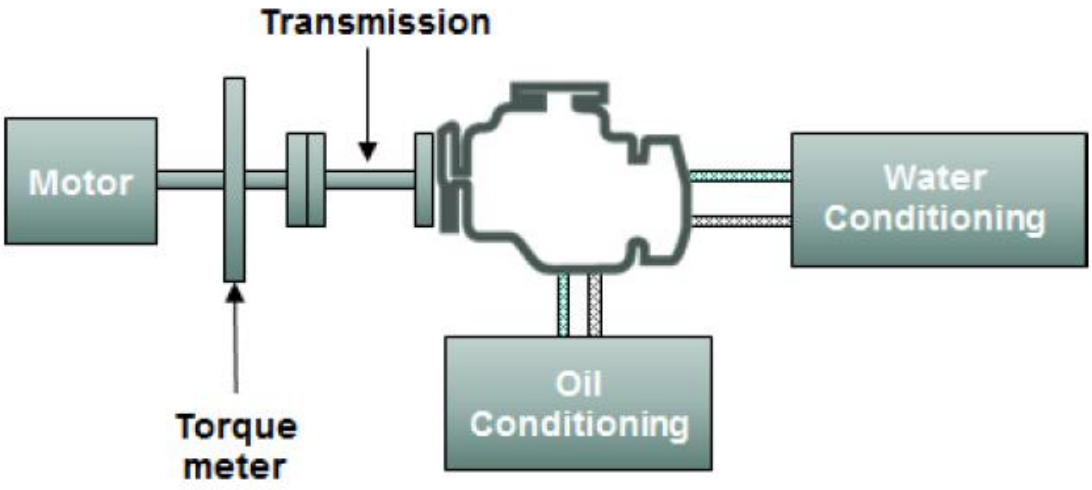

Figure 1. Test bench configuration for motored tests.

In the FTT, the engine is motored via an electrical dynamometer connected through direct shaft to the engine crankshaft. A high precision torquemeter (with an accuracy of ± 0.1 N·m) is located along the shaft. Friction torque measurements are obtained from the dynamometer output torque necessary to maintain engine rotation given engine speeds and oil/coolant temperatures. This setup is detailed in Figure 1 and is known to achieve maximum accuracy and flexibility for friction torque measurements, with significance threshold proven at 0.6% of total friction torque measured (with 95% confidence).

The motored test was performed following the protocol:

- Firstly, the engine was installed with spark plugs, fuel injectors, exhaust and intake manifold removed, hence there is no compression force during the test. It is worth mentioning that the unit employed in this test is a used one, close to what is considered the end of the useful life of the engine. The purpose of this, is to assess the influence of MoDTC additive in a unit which has already undergone a noticeable degree of wear in its parts.
- As mentioned above one lubricant with MoDTC and its correspondent equivalent without MoDTC were used. These oils were tested at different engine speeds listed in Table 2. Torque is averaged over 10 minutes at each of the tested speeds. Before testing any candidate oil, two flush runs were conducted to remove all chemical traces of previously tested oils. The oil filter is changed following each flush with this protocol to prevent cross-contamination.
- The engine was run at all times maintaining the oil temperature at 110 °C. Fluid temperatures are regulated with specific oil and water conditioning units within ±0.1 °C accuracy. The test rig, despite being not equipped with AHU (Air Handling Unit), ensured an intake air temperature regulation around ±1 °C thanks to a control loop using a sensor located in test bed air intake. In

parallel, additional sensors were installed for atmospheric pressure and hygrometry measurements.

Table 2. FFT operation conditions.

Step	Temperature	Speed	Lubricant
F1.1	Flush: Previous to experiments - 1st run		
F1.2	Flush: Previous to experiments - 2nd run		
1.1	110 °C	4400	5W30
1.2		3500	
1.3		3000	
1.4		2500	
1.5		2000	
1.6		1500	
1.7		1000	
F2.1	Flush: Previous to MoDTC addition - 1st run		
F2.2	Flush: Previous to MoDTC addition - 2nd run		
2.1	110 °C	4400	5W30+1%MoDTC
2.2		3500	
2.3		3000	
2.4		2500	
2.5		2000	
2.6		1500	
2.7		1000	

After the test the engine was disassembled and the parts visually inspected. All the parts that underwent wear were cleaned with heptane to remove the excess of oil and analysed using Raman microscopy and Scanning Electron Microscopy (SEM) to resolve the products from tribochemistry of MoDTC additive. When required, the samples were cut to size, making sure that the area of analysis was not affected either by contaminants, or by heat.

Raman spectra was obtained on the samples at the areas of interest identified by the built-in microscope, in order to identify the locations populated with MoS_2 and other molybdenum-containing species, which depend on the contact conditions and the materials of the surfaces. SEM analysis provided additional information on the materials involved and the wear mechanisms. The variability of materials used in the engine studied in this work is presented in Table 3.

For the Raman analysis, an in-via Reflex Renishaw Raman microscope equipped with a 488 nm laser, a 2400 lines/mm grating, and a Leica microscope with both 50x

and 50x long working distance objectives, was used to analyse the parts. Sufficient acquisition time was employed to collect the spectra. A maximum laser intensity of 10% was applied, delivering a power of 1 mW on the sample, to ensure no damaged is produced on the samples. The lateral resolution under the current configuration was around 1 µm, and the spectral resolution 1 cm^{-1}.

Table 3. Summary of the different materials and coatings used in the engine.

System	Part	Material
Cam-Follower	Camshaft	Cast Iron
	Lifter (Bucket type) top surface	taC-DLC (tetrahedral amorphous carbon DLC)
	Lifter (bucket type) internal surface	Steel, chromium coated.
	Valve stem	Steel
Piston-Cylinder	1st ring	taC-DLC coated
	2nd ring	Phosphate coated
	Oil ring	taC-DLC coated
	Oil skirt	Carbon based coating
	Cylinder liner	Steel
Other	Gudgeon pin	Steel
	Bearing insert	Multilayer, contains Bi
	Timing chain	Hardened steel
	Oil pump vanes	Steel

A Hitachi TM3030 Plus SEM equipped with an Oxford Instruments EDX microprobe is use to determine the wear mechanisms and elemental composition of representative parts.

3. Results and Discussion

3.1. Torque Measurements

Figure 2 depicts torque values measured during the motored test for both oils over a range of different speeds. The difference between the performances obtained with both oils is plotted as a percentage value. At high speed, friction reduction is in the 0.5-1.5% range, showing limited influence of the MoDTC additive. At lower speeds (below 2000 rpm) the decrease of torque values is larger, reaching a maximum value of almost 2.5% torque reduction at the minimum speed measured, 1000 rpm.

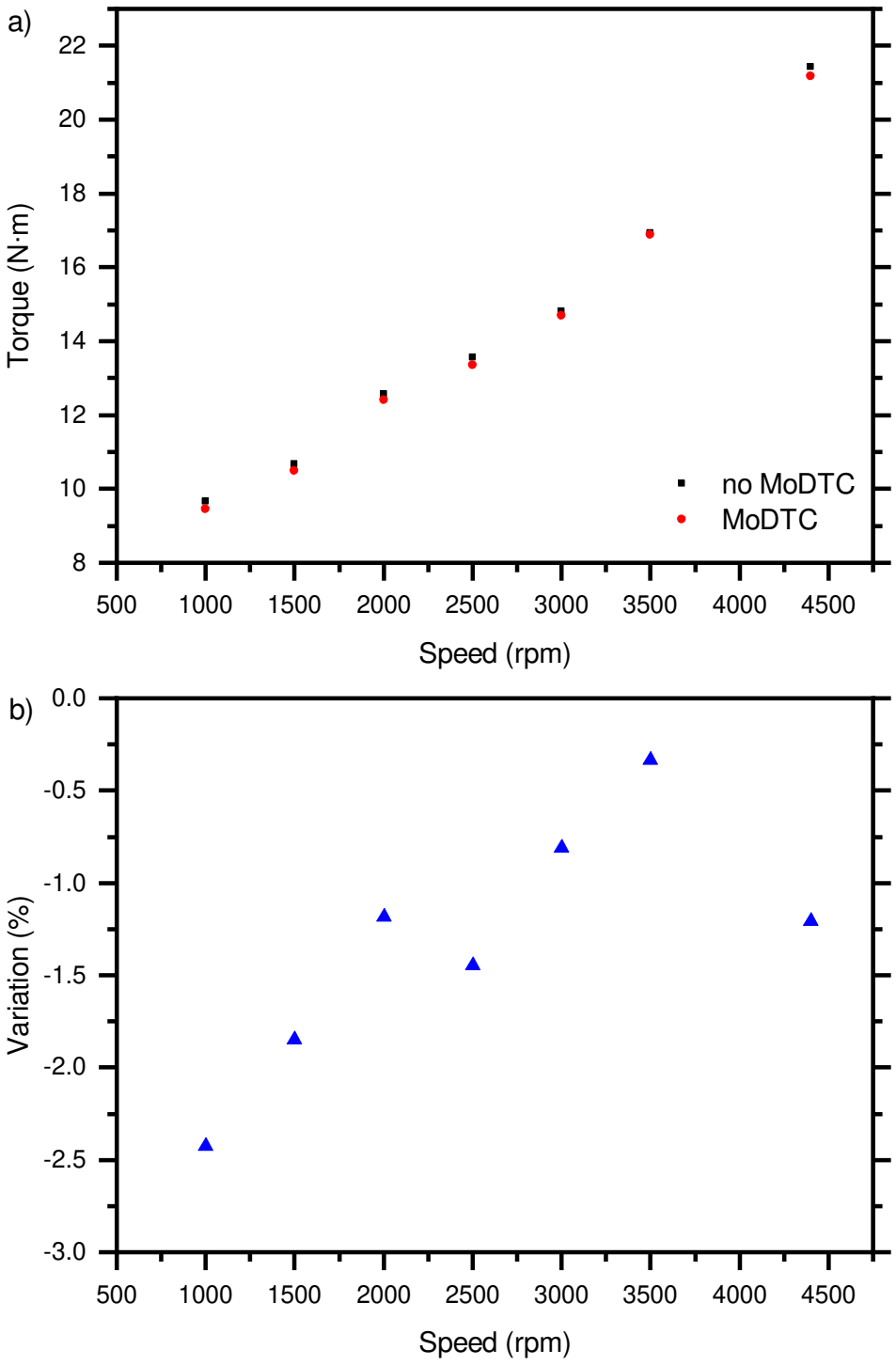

Figure 2. a) Torque vs speed for FF oil and MoDTC-FF oil. b) Variation in percentage of friction torque, representing a reduction of frictional losses.

The larger reduction in torque measurements using the MoDTC-FF-oil at low speeds with respect to higher speeds can be easily explained by the fact that at lower speeds more tribological contacts inside the engine meet the boundary lubrication regime [22, 23]. Thus, MoDTC can excel at reducing friction, as boundary lubrication regime is required for this additive to function as a friction modifier.

3.2 Surface analysis

Every surface undergoing wear inside the engine has been analysed. In this section results from several parts are presented according to the system they belong. Raman microscopy has been introduced as the main characterisation tool for this work, as it can accurately detect the presence of the solid lubricant MoS_2, manifested by two peaks at 380 cm^{-1} and 410 cm^{-1} namely E^1_{2g} and A_{1g} [18, 24]. Other molybdenum species of interest can be detected with this technique, such as amorphous MoS_x (320 cm^{-1} and 520 cm^{-1} broad bands) [25, 26], $FeMoO_4$ (926 cm^{-1}) [27], MoO_3 (991 cm^{-1}) [28], as well as other species formed on the surface, such as oxides, phosphates, etc.

Cam-follower system

As previously mentioned, the cam-follower system consists of a direct acting system, where the camshaft during its rotary movement directly presses the followers (buckets) that displace the valves, controlling the aperture time and the gasses admission/exhaust to/from the combustion chamber.

Particularly, the parts under investigation in the cam-follower system are the following: the camshaft lobes, bucket followers, and valves. These three parts constitute the contact pathway that enables the aperture of the valves in a direct acting system.

Under visual inspection, the camshaft lobe exhibits a tribofilm in the nose area, ranging ±15 degrees in the angular direction with respect to the tip of the lobe, and the entire width of the lobe in the axial direction, except for the last 1mm distance area towards both edges. MoS_2 is present in most part of the tribofilm, with the amount being greater towards the tip and the central part of the lobe in the axial direction. The reason why no tribofilm is found at the edges in the axial direction (Figure 3a) could be related to lower contact pressure in the area towards the edge [29] or the growth of the fluid film thickness at this zone [30], shifting the lubrication regime to hydrodynamic in this part of the contact. The cam was also analysed as a function of the angular position in the central part of the cam. As noticed earlier, the tribofilm can be observed in the ±15 degrees range, in agreement with other direct acting cam-follower systems tested on single cam-follower rigs [31]. However, MoS_2 is only present up to 7 degrees from the topmost part, as shown in Figure 3b, where higher contact pressures are achieved between the cam and the bucket, differing from other work where MoS_2 was found in a wider angular range [32]. Differences in working conditions, oil formulation, cam profile and matching materials could be responsible for these differences.

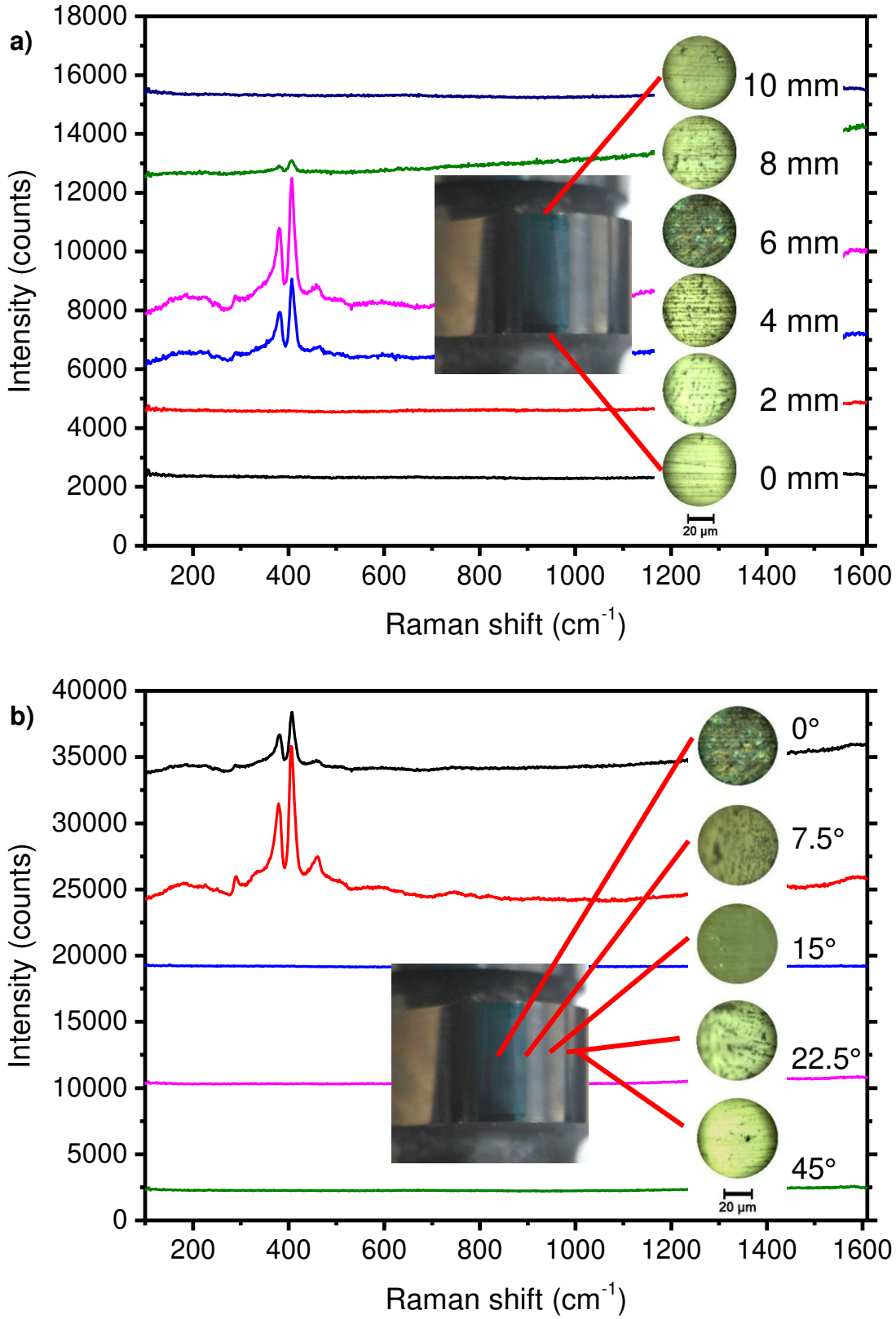

Figure 3. Raman spectra obtained in the a) axial and b) angular direction of the engine camshaft lobe. Spectra have been shifted for clarity.

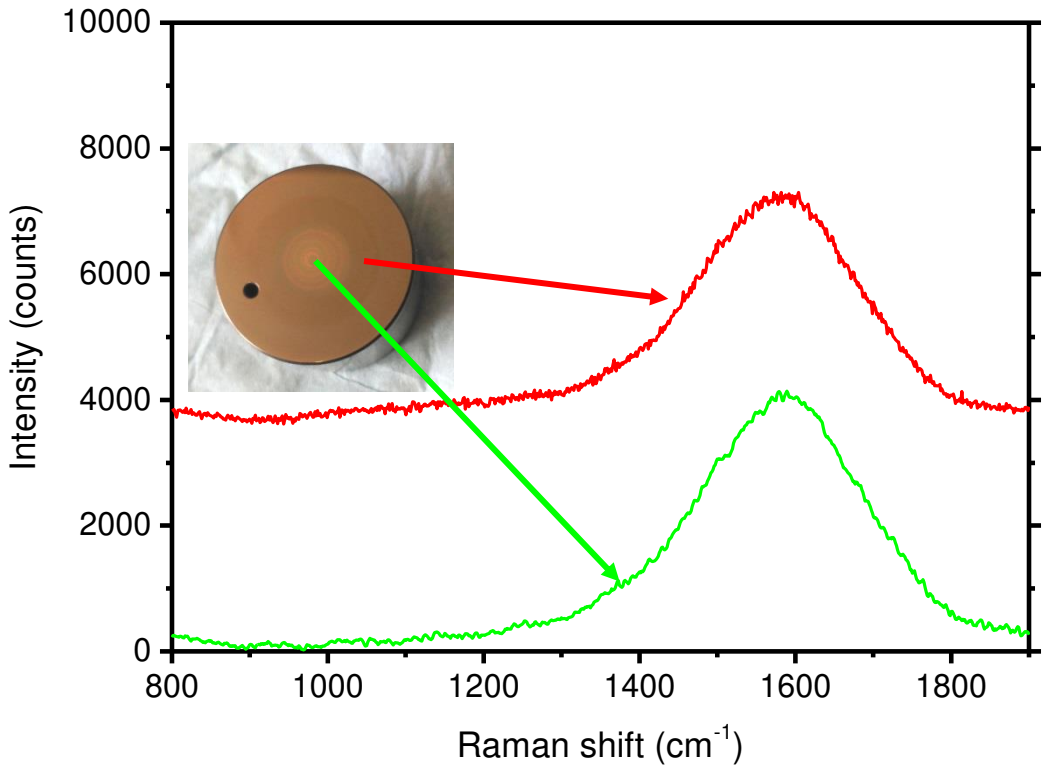

Figure 4. Raman spectra of a taC-DLC coated bucket after test. Spectra have been shifted for clarity.

As for the part in direct contact with the cast-iron cam-shaft, the non-hydrogenated taC-DLC coated bucket, no measurable wear or tribofilm were detected on the buckets after the tests, as a contrast to what was found in the ferrous counterface. It is well-known that DLC are not very active towards the tribofilm formation from additives that are designed to run in ferrous systems, leading to very thin or no tribofilm when fully formulated engine oils are used [33, 34].

The highest contact pressure is produced at a certain distance from the centre, half way between the centre and the edge of the bucket, reaching 800 MPa high contact pressure [29]. This contact pressure is not high enough to promote the delamination of the coating. During the test, no wear is produced in this part. Only a slight change in colour can be detected in the maximum contact pressure area, suggesting structural change in the coating top layer or the sub-layer. The taC-DLC did not produce a tribofilm on the tappet, moreover, no change in DLC structure was found in this part (Figure 4). This fact agrees what has been experimentally found in previous work, when using a molybdenum-containing fully formulated oil in a 1GPa contact pressure pin-on-disk test produced MoS_2 tribofilm formation on steel surfaces but not in non-hydrogenated DLC coated parts [4].

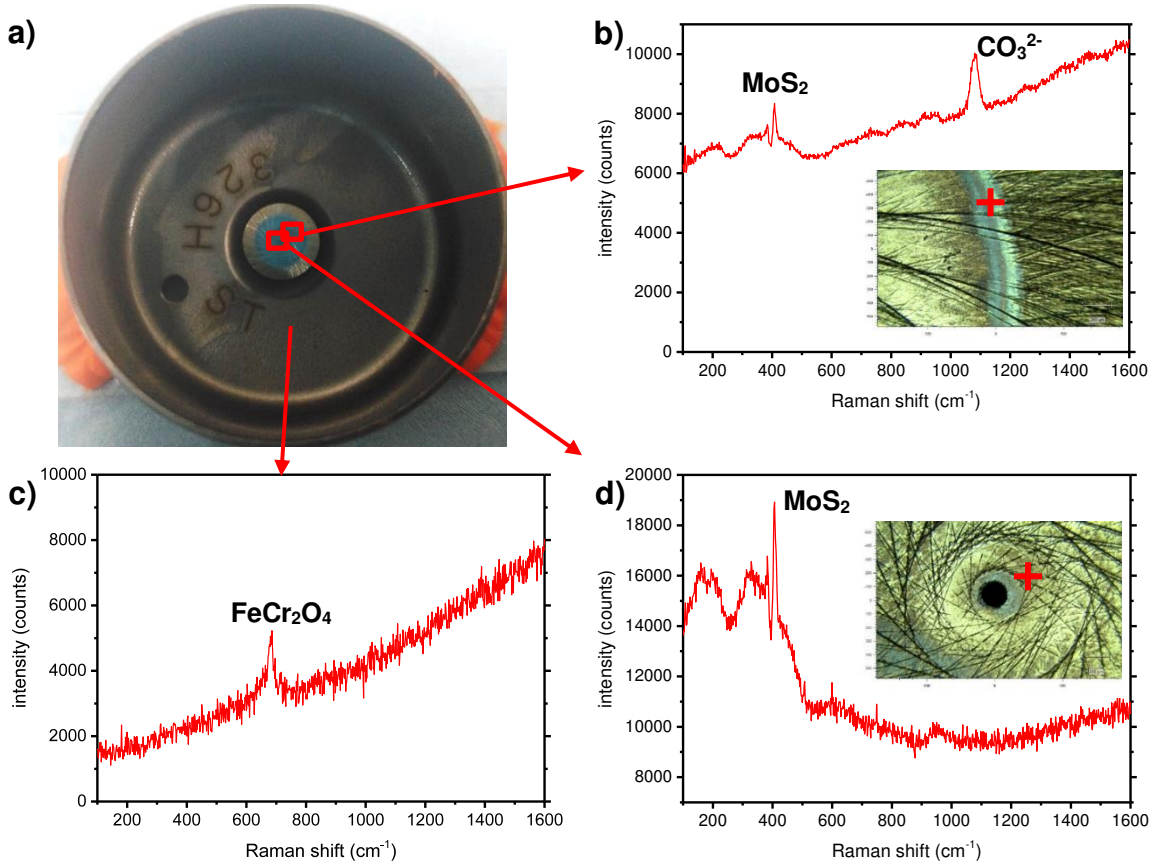

Figure 5. Raman analysis on bucket underneath surface.

The tappets have other surfaces in contact and relative motion besides the bucket crown analysed above. Under the bucket, which is chromium coated, there is a central protuberance which contacts the top part of the valve stem. This part has a characteristic spiral crosshatch pattern that most likely promotes the bucket rotation. Raman analysis on this part shows the presence of a tribofilm containing MoS_2 and carbonates on this surface (Figure 5b and d). It is worthwhile pointing out the formation of this friction-reducing tribofilm on a surface consisting of chromite, $FeCr_2O_4$, which is different from steel/cast iron surfaces where MoS_2 tribofilm is usually formed under boundary lubrication. The presence of this low-friction tribofilm, could not only affect the friction losses in the bucket/valve interface, but also modify the rotation speed of bucket. According to literature, FM reduces the rotation speed at high temperature, where mixed to boundary lubrication regimes dominate in the system [35]. However, in another study the addition of MoDTC to a fully formulated oil leads to an increase in the speed rotation [36]. Nevertheless, predicting the rotating speed is challenging, as the speed depends on the cam/tappet, tappet/valve and tappet/bore contacts [37]. In the present study no significant wear or tribofilm were found in the bore part of the tappet, suggesting this contact is working under hydrodynamic regime. Hence the rotation of the tappet would be dominated by the camlobe/tappet crown, and the under tappet/valve contacts.

The valve has also been studied in the present work. No signs of MoS_2 were found in the top part of the valve stem.

Piston-liner system

The engine piston assembly contains three rings in contact with the cylinder bore; namely the first ring, the second ring and the oil ring. All three rings are coated. The counterface of these rings is a ferrous liner embedded in the aluminium engine block. Ferrous surfaces play a role in the effectiveness of both friction modifiers and antiwear additives [8, 24, 38].

The main parts undergoing wear or tribofilm formation are the cylinder bore (a ferrous liner), the ring pack (first ring, second ring and oil ring) and the piston skirt, evidencing boundary lubrication regime at some point during the engine cycle.

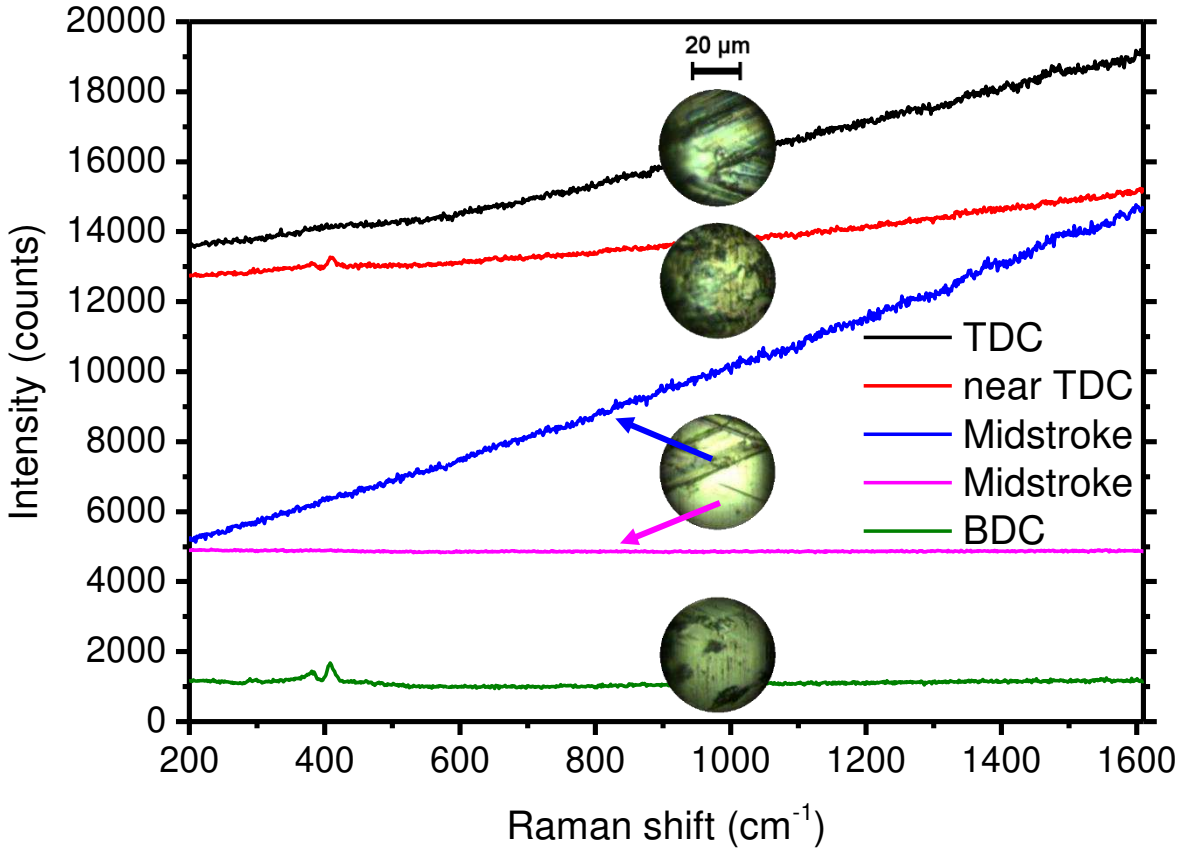

Figure 6. Raman spectra of cylinder liner at different stroke points. Spectra has been shifted for clarity.

With regards to the liner, shown in Figure 6, interesting features are found as a function of the stroke position. Above the top dead centre (defined as the topmost point where the first ring is in contact with the liner), only very strong fluorescent signal is detected by Raman. This fluorescence is produced by the soot-like carbon generated by the thermal degradation of the engine oil during the test [39, 40], as high temperatures generated by high compression of the air produce the decomposition of the oil dragged onto that part of the cylinder. At the top dead centre area, where the ring pack meets the highest position, fluorescence and occasionally MoS_2 is detected. The latter is especially found in the vicinity of the top dead centre, at 8 mm, where the oil ring stroke finishes in its reciprocating movement. In the middle part of the stroke fluorescence is detected again at some patches located in particular places following

the irregularities of the liner caused by the honing process. In this case, the Raman features are similar to those obtained with FF oils in tribometer bench tests [4]. At smoother areas, no tribofilm or Raman signal are detected. In this part of the stroke no MoS_2 signal is detected, regardless of the topography, suggesting that MoS_2 can only be formed if boundary lubrication regime is achieved. At the bottom part of the stroke, a patchy but clear MoS_2 containing tribofilm is detected. No fluorescence is found in this part of the cylinder. Generally speaking, fluorescence is stronger towards the top part of the cylinder and lower towards the bottom part, in agreement with the higher temperature promoting the degradation of the engine oil.

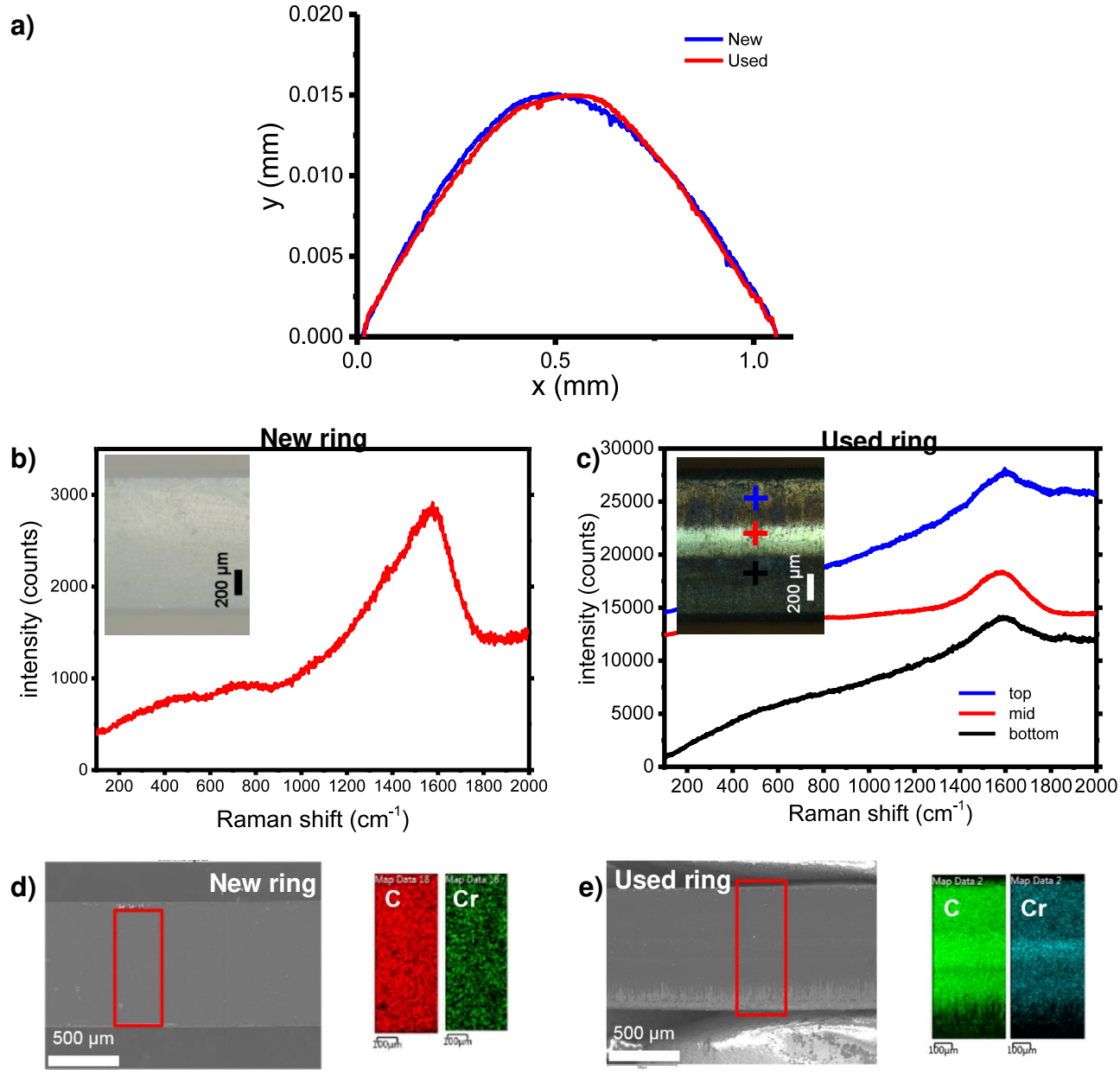

Figure 7. a) Profilometry, b and c) Raman microscopy, d and e) SEM micrograph/EDX mapping of new and used first ring.

In this part of the section, as-received new rings have been analysed for comparison purposes.

Figure 7 shows a comparative study on the first ring (compression ring) condition between as-received and after the FTT. To begin with, wear volume is too low to be measured by profilometry (Figure 7a). Raman microscopy, shown in Figure 7b and c, confirms that taC-DLC features are kept across the bore edge, with minor differences in the spectrum background, due to the deposition of a very thin tribofilm at both sides of the central part of the ring. Further analysis using SEM-EDX (Figure 7d and e) demonstrates this fact, and shows that a very slight thinning of the coating in the central part of the ring might be produced, as more chromium belonging to the CrN coating interlayer is revealed by EDX. As with the non-hydrogenated taC-DLC on the tappet, no MoS_2 is formed or transferred onto this surface.

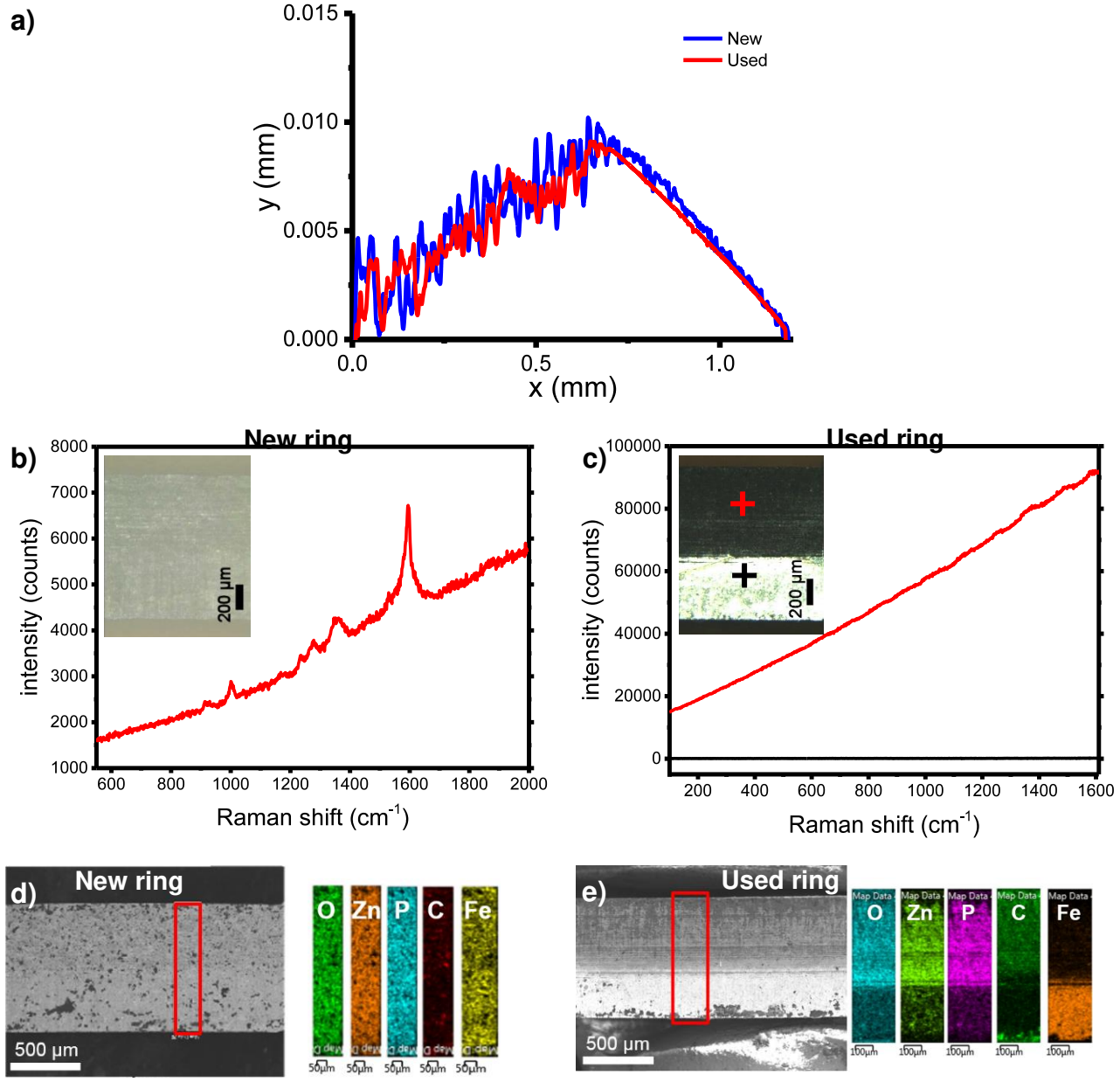

Figure 8. a) Profilometry, b and c) Raman microscopy, d and e) SEM micrograph/EDX mapping of new and used second ring.

As for the second ring, wear volume determination is again not feasible, as the roughness of the sample across the bore edge overshadows the global height differences (Figure 8a). However, a clear polishing is seen at the bottom part of the ring, demonstrated by a visible change in roughness. Moreover, both microscope images (Figure 8b and c) and SEM images (Figure 8d and e) confirms that the coated surface is polished out in the bottom part of the ring. The coating, consisting of zinc phosphate (peak at 1000 cm^{-1}) and low ordered graphitic carbon (see peaks around 1350 and 1600 cm^{-1} in Figure 8b) is worn out, revealing the non-Raman sensitive ferrous material underneath. Interestingly, no MoS_2 is formed in this ferrous part of the second ring, suggesting that despite undergoing boundary lubrication, a set of contact conditions (contact pressure, speed, time throughout a cycle undergoing asperity to asperity contact, etc.) is needed for MoDTC to MoS_2 formation.

The oil control ring consists of a tandem of rings separated by an undulated spacer. These ring elements are manufactured with a taC-DLC coating of the same nature than that of the first ring or the top part of the tappet. Figure 9a shows the ring element bore edge profile evidencing a noticeable amount of wear volume, showing a flattening/polishing of the central part of the round profile. Raman microscopy (Figure 9b and c) confirms that in this central part, the DLC coating has been removed, revealing a non-Raman sensitive surface. Further EDX analysis (Figure 9d and e) shows the presence of chromium in the worn area, indicating the exposure of the CrN interlayer. Similarly to other coated parts, no MoS_2 was found. Although MoDTC has been previously reported as the source of excessive chemical wear of DLC materials [4, 41, 42], the non-hydrogenated nature of the coating, and the fact that neither the first ring nor the tappet exhibited accelerated wear, suggest that in this case excessive contact pressure could have promoted more wear in this specific component.

The Al-Si alloy piston skirt, which also enters in contact with the liner, has a carbon based coating applied on the piston grooved surface. There is a degradation of this coating, as well as some abrasion lines in the stroke direction (perpendicular to the grooves). Raman microscopy did not show any differences in the worn area in terms of composition, but a physical removal of the low friction coating, demonstrated by wider uncoated stripes (see micrograph insets and Raman spectra in Figure 10a and b), that reveal the Raman crystalline silicon band at 521 cm^{-1}. The chemical structure of the coating could not be evaluated due to the strong fluorescence background. In this particular case, no MoS_2 was found on the coating, or on the aluminium alloy part, despite being this substrate suitable to support MoS_2 formed by tribochemistry of MoDTC [43].

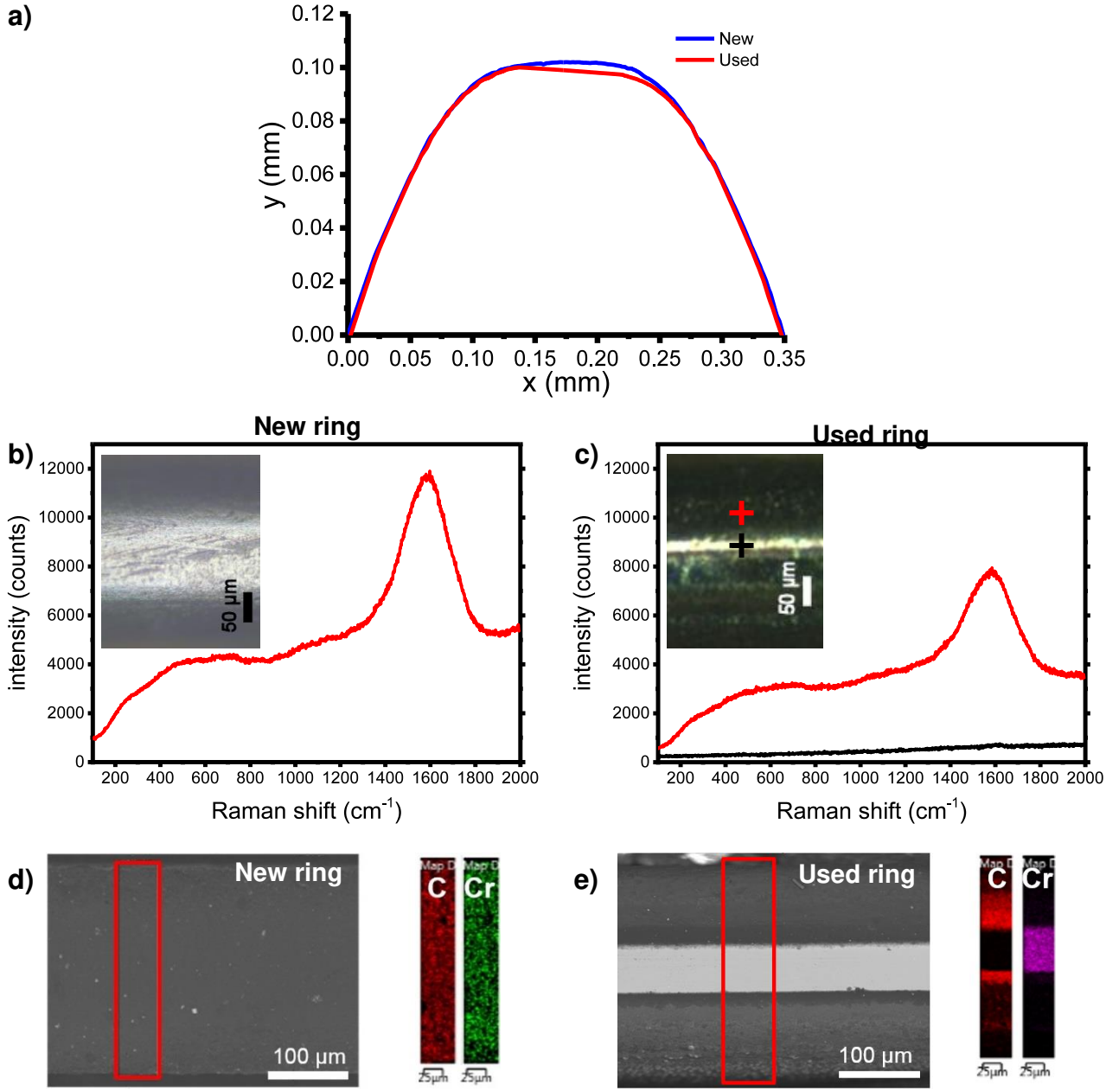

Figure 9. a) Profilometry, b and c) Raman microscopy, d and e) SEM micrograph/EDX mapping of new and used oil ring.

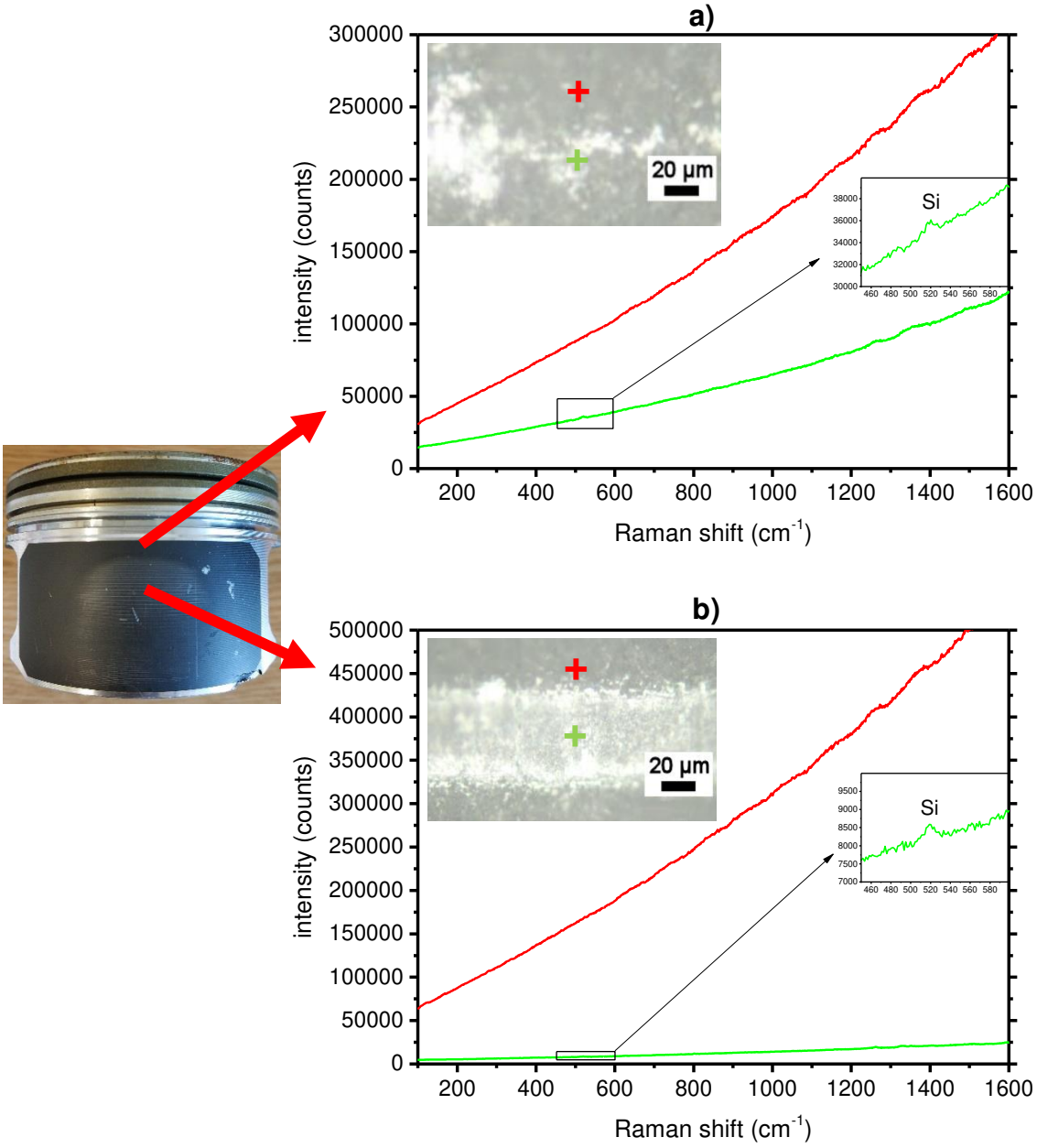

Figure 10. Raman spectra of piston skirt at two different locations. a) Unworn area. b) Worn area.

Piston-Connecting rod-Crankshaft system

In the engine under study, the gudgeon pin is fixed to the connecting rod. Hence, the tribological contact occurs between the steel pin and the aluminium piston head. Slight abrasion lines, and a sparse tribofilm (antiwear tribofilm with a characteristic 667 cm^{-1} Fe_3O_4 Raman peak [44]) formed are indicative of a very mild tribological contact that does not promote MoS_2 on the surface, as demonstrated by the absence of the MoS_2 peaks using Raman microscopy (Figure 11).

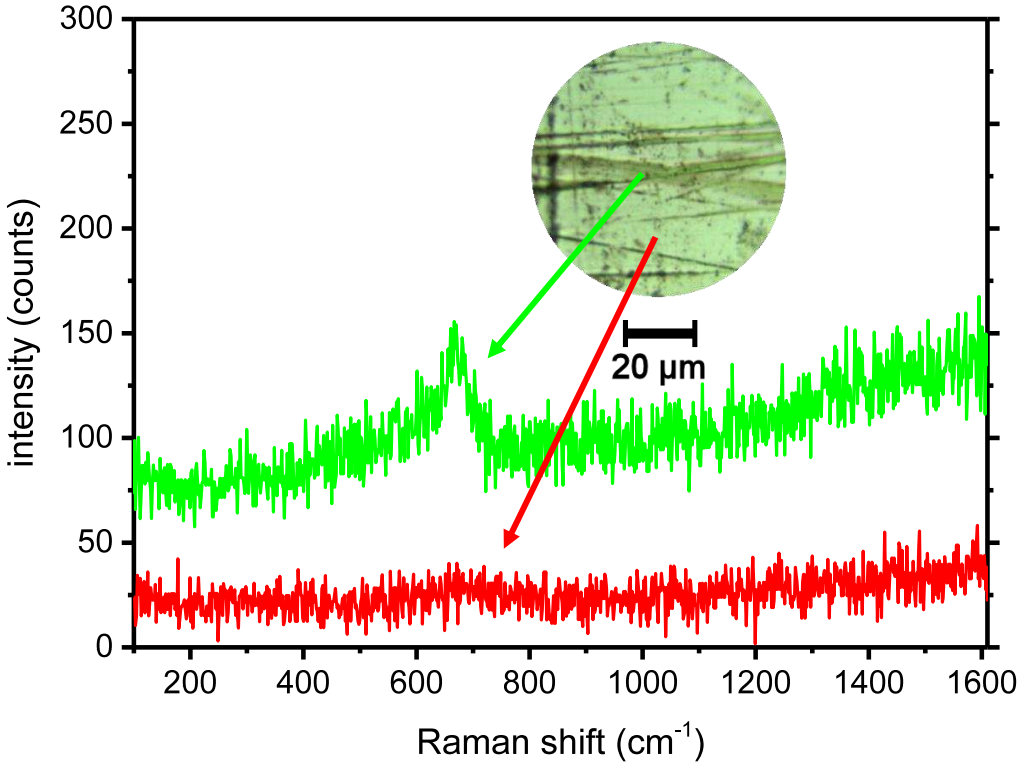

Figure 11. Raman microscopy of gudgeon pin.

At the other end of the connecting rod, plain bearings and the crankshaft work under hydrodynamically supporting forces in rotational movement, hence they do not enter the boundary lubrication regime unless starvation occurs. The connecting rod plain bearing insert exhibits abrasion lines in the sliding direction (probably due to third body wear), and deformation of the bearing material in the central part of the plain bearing. This level of damage is found in this sort of engine tests [45]. As expected, no MoS_2 was found.

Other parts

Apart from the three main tribological systems considered in the engine (piston-liner, cam-follower and crankshaft-connecting rod-piston head), tribological contacts may occur in other suitable places. There are for example symptoms of wear in the chain links (silent timing chain type) and in the oil pump vanes (from a rotary vane oil pump).

The chain pins, which hold the links together, exhibit wear (smooth, slight polishing). In this area, a very patchy thin tribofilm is present. Raman analysis (Figure 12) shows iron oxide (magnetite), hydrocarbons and probably amorphous iron sulphides (band at 280-300 cm^{-1}), these chemical species are common in anti-wear tribofilms [40]. No MoS_2 is found in this case, most probably because no true boundary lubrication is achieved at this location.

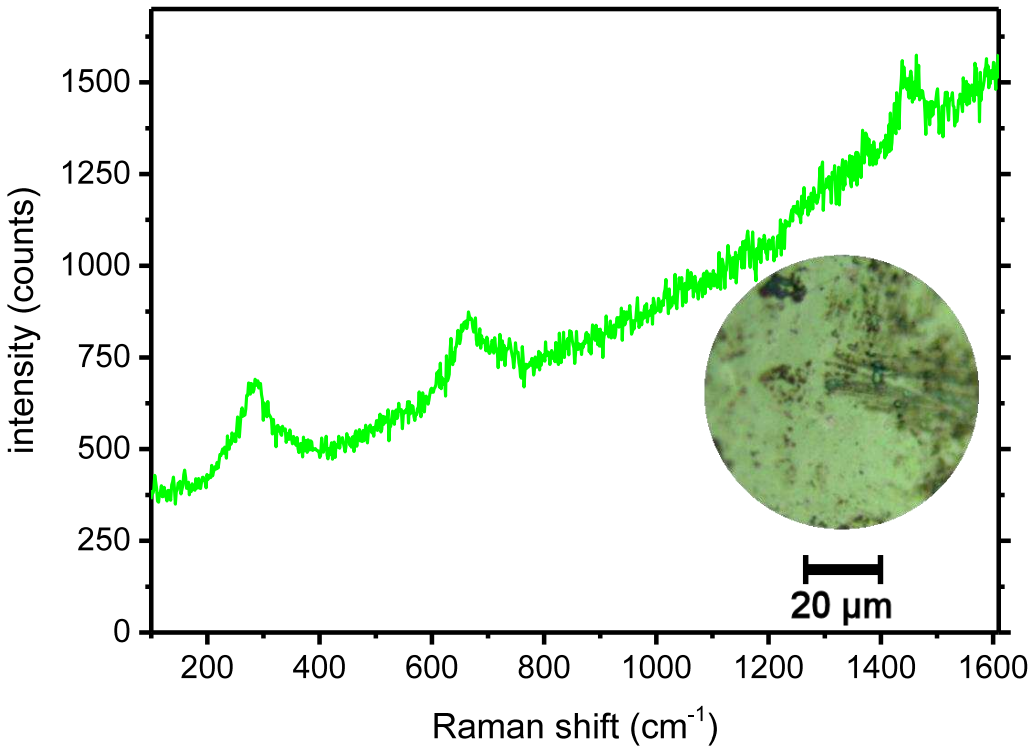

Figure 12. Raman microscopy of timing chain link.

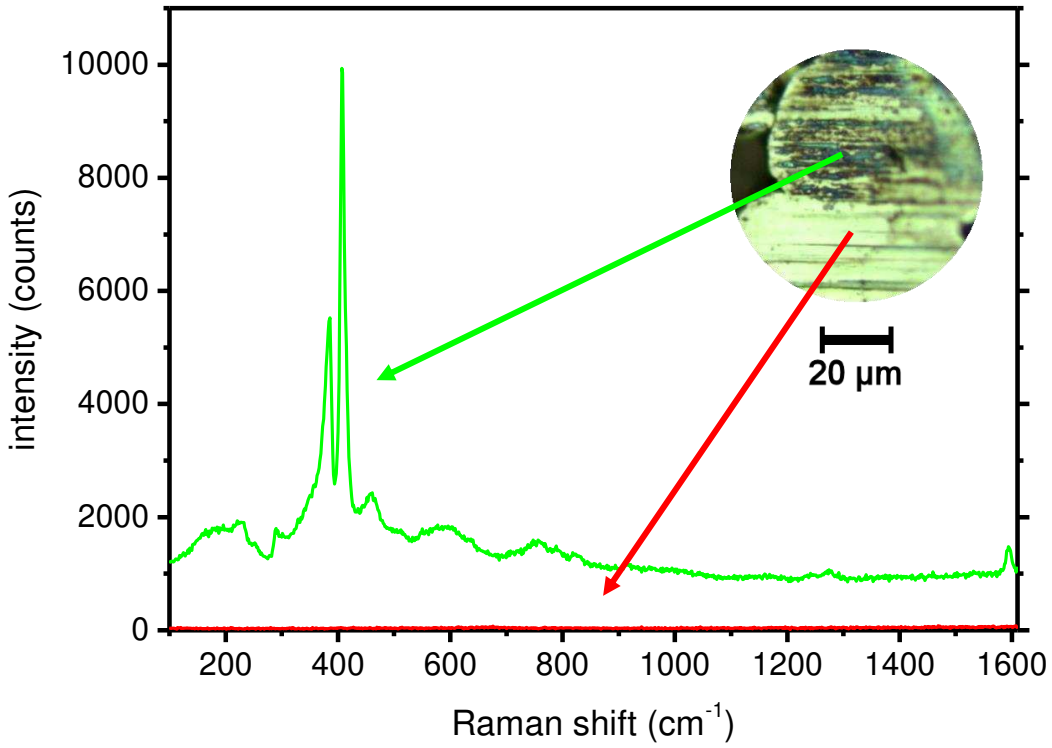

Figure 13. Raman microscopy of the pump vane tribofilm at its bore edge.

As for the variable oil pump, a different situation is found. A patchy, MoS_2 rich tribofilm is present on oil pump vanes, in particular, at the edges in contact with the

pump bore, and the areas in contact with the rotor, as shown in Figure 13. MoS_2 presence in this location helps reducing the losses produced by the oil pump. This component can be responsible for up to 10% of all mechanical friction losses [46], and its fuel consumption boundary potential can reach 1%, which is in the same range of the piston skirt contribution to the engine fuel utilisation [47].

Table 4. Summary of the Raman results on different engine parts.

System	Subsystem	Found usually	Found occasionally	Notes
Cam-Follower	Cam lobe	MoS_2	Fluorescence	MoS_2 is only found at the tip of the camlobe, where BL is expected.
	Tappet	taC		No tribofilm is found
	Tappet-Under	MoS_2	Phosphates	
	Valve	Fluorescence		No MoS_2 is found
Piston-Cylinder	1st ring	taC		
	2nd ring	Fluorescence		The Raman fluorescent coating is worn out at the lower part. New parts show graphitic structures and phosphates.
	Oil ring	taC		ta-C is worn out in the central part
	Skirt	Fluorescence. Si from Al alloy		Worn areas showed higher presence of silicon, and less fluorescence. No tribofilm.
	Cylinder Liner	MoS_2	Fluorescence	Fluorescence is especially found in the top part of the liner, whereas MoS_2 is found in both stroke ends, where BL is expected. In mid-stroke region Raman sensitive tribofilm is only formed at honed abrasion lines.
Piston-Connecting Rod-Crankshaft	Gudgeon Pin	No signal	Fe_3O_4	
	Plain Bearing	Bismuth		
Other	Pump vane	MoS_2		
	Time chain link	No signal	Sulphides, Fe_3O_4	

Summary of Raman results

In this project, Raman spectroscopy in combination with other techniques, has been used on a large variety of engine components working at different lubrication regimes, having different chemical compositions and shapes, whilst being lubricated with the same oil.

In Table 4, the main Raman findings are summarised. MoS_2 was found at locations were iron containing surfaces and boundary lubrication conditions were met. DLC coatings did not undergo apparent graphitisation or chemical degradation, but excessive wear occurred in some areas. The interaction between oil and surfaces was evident.

It is worth to mention that even if the main focus was on the formation of the very Raman sensitive low friction MoS_2 tribofilm, additional information has been obtained, such as the confirmation of coating materials and removal of coatings, evidences of structural changes and hydrocarbon absorption in some parts, as well as the formation of antiwear film in others, being fluorescence the main limitation of this technique.

4. Conclusions

The present work is an attempt to assess the influence of molybdenum based additives in the frictional performance of engines by using motored tests and analytical characterisation techniques. For the first time, a comprehensive analysis using Raman microscopy has been carried out covering most of the engine parts in tribological contact.

The addition of 1% MoDTC (1000 ppm Mo) leads to a friction reduction across the full engine speed range. Its impact is higher at lower speeds (1000 rpm), where more boundary lubricated contacts are expected. At this speed regime, up to 2.5% of friction torque reduction is achieved. Raman microscopy shows the presence of the solid lubricant MoS_2 promoted from MoDTC tribochemistry on the tribological surfaces at specific locations within the engine. This specie is found in contacts where boundary lubrication, ferrous surface and relative high contact pressure are met, such us the returning points in the liner belonging to the piston-cylinder tribosystem and the camshaft lobe in the direct acting cam-follower system. Other areas, such as the vanes of a variable oil pump, do have MoS_2 formed by tribochemical processes. The formation of a low friction tribofilm at very specific locations within the engine explains the torque reduction when MoDTC is used, showing the huge impact of tribochemistry if we consider the small amount of area affected by this additive within the engine.

This paper sets up the basis for the assessment of molybdenum based friction modifiers in full engine tests, both motored and fired. On-going work is oriented towards the assessment of organic molybdenum tribochemistry on fired engines, confirming the suitability of Raman analysis in motored tests for performance prediction in fired test. There are also continuing actions oriented to the quantification of MoS_2 low-friction tribofilm and its relation to friction performance.

Acknowledgements

The authors wish to thank Total Marketing Services and the EPSRC for funding the present work.

References

1. SAE International, *J300_201501 Engine Oil Viscosity Classification*. 2015.
2. Graham, J., H. Spikes, and R. Jensen, *The Friction Reducing Properties of Molybdenum Dialkyldithiocarbamate Additives: Part II - Durability of Friction Reducing Capability.* Tribol. Trans., 2001. **44**(4): p. 637-647. DOI: 10.1080/10402000108982505.
3. Farr, J.P.G., *Molybdenum disulphide in lubrication. A review.* Wear, 1975. **35**(1): p. 1-22. DOI: 10.1016/0043-1648(75)90137-4.
4. Espejo, C., et al., *MoDTC Tribochemistry in Steel/Steel and Steel/Diamond-Like-Carbon Systems Lubricated With Model Lubricants and Fully Formulated Engine Oils.* J. Tribol., 2019. **141**(1): p. 012301-012301-12. DOI: 10.1115/1.4041017.
5. Neville, A., et al., *Compatibility between tribological surfaces and lubricant additives—How friction and wear reduction can be controlled by surface/lube synergies.* Tribol. Int., 2007. **40**(10–12): p. 1680-1695. DOI: 10.1016/j.triboint.2007.01.019.
6. Kosarieh, S., et al., *Tribological performance and tribochemical processes in a DLC/steel system when lubricated in a fully formulated oil and base oil.* Surf. Coat. Technol., 2013. **217**(0): p. 1-12. DOI: 10.1016/j.surfcoat.2012.11.065.
7. Vengudusamy, B., et al., *Tribological properties of tribofilms formed from ZDDP in DLC/DLC and DLC/steel contacts.* Tribol. Int., 2011. **44**(2): p. 165-174. DOI: 10.1016/j.triboint.2010.10.023.
8. Vengudusamy, B., et al., *Behaviour of MoDTC in DLC/DLC and DLC/steel contacts.* Tribol. Int., 2012. **54**(0): p. 68-76. DOI: 10.1016/j.triboint.2012.04.028.
9. ASTM International, *ASTM G99-17, Standard Test Method for Wear Testing with a Pin-on-Disk Apparatus*. 2017: West Conshohocken, PA.
10. ASTM International, *ASTM G133-05(2016), Standard Test Method for Linearly Reciprocating Ball-on-Flat Sliding Wear*. 2016: West Conshohocken, PA.
11. Khaemba, D.N., et al., *The role of surface roughness and slide-roll ratio on the decomposition of MoDTC in tribological contacts.* J. Phys. D Appl. Phys., 2017. **50**(8): p. 085302. DOI: 10.1088/1361-6463/aa5905.
12. Heath, D.H., et al. *ASTM's Development of the Sequence VI Fuel Efficient Engine Oil Dynamometer Test*. in *International Fall Fuels and Lubricants Meeting and Exposition*. 1987. Toronto, ON, Canada: SAE Technical Paper 872120. DOI: 10.4271/872120.
13. Noorman, M.T., et al. *Overview of Techniques for Measuring Friction Using Bench Tests and Fired Engines*. in *International Spring Fuels and Lubricants*

Meeting and Exposition. 2000. Paris, France: SAE Technical Paper 2000-01-1780. DOI: 10.4271/2000-01-1780.

14. Chamberlin, W.B. and T.J. Sheahan. *Automotive Fuel Savings Through Selected Lubricants*. in *Automotive Engineering Congress and Exposition*. 1975. Detroit, MI, USA: SAE Technical Paper 750377. DOI: 10.4271/750377.
15. Hanada, K., et al. *Development of a Valve Train Wear Test Procedure for Gasoline Engine Oil*. in *International Congress and Exposition*. 1994. Detroit, MI, USA: SAE Technical Paper 940794. DOI: 10.4271/940794.
16. Taylor, M.P. *The Effect of Gas Pressure on Piston Friction*. 1936. SAE Technical Paper 360117. DOI: 10.4271/360117.
17. Styer, J. and G. Guinther, *Fuel Economy Beyond ILSAC GF-5: Correlation of Modern Engine Oil Tests to Real World Performance.* SAE Int. J. Fuels Lubr., 2012. **5**(3): p. 1025-1033. DOI: 10.4271/2012-01-1618.
18. Khaemba, D.N., A. Neville, and A. Morina, *A methodology for Raman characterisation of MoDTC tribofilms and its application in investigating the influence of surface chemistry on friction performance of MoDTC lubricants.* Tribol. Lett., 2015. **59**(3): p. 1-17. DOI: 10.1007/s11249-015-0566-6.
19. Xu, D., et al., *Understanding the Friction Reduction Mechanism Based on Molybdenum Disulfide Tribofilm Formation and Removal.* Langmuir, 2018. **34**(45): p. 13523-13533. DOI: 10.1021/acs.langmuir.8b02329.
20. Kobayashi, A., et al. *Development of New I3 1.2L Supercharged Gasoline Engine*. in *SAE 2012 World Congress & Exhibition*. 2012. Detroit, MI, USA: SAE Technical Paper 2012-01-0415. DOI: 10.4271/2012-01-0415.
21. JASO, *M 365:2019 Automobile Gasoline Engine Oils - Motored Fuel Economy Test Procedure*. 2019, JASE.
22. Gangopadhyay, A., E. Soltis, and M.D. Johnson, *Valvetrain friction and wear: Influence of surface engineering and lubricants.* Proc. Inst. Mech. Eng. Part J J. Eng. Tribol., 2004. **218**(3): p. 147-156. DOI: 10.1177/135065010421800302.
23. Yamamoto, K. and Y. Moriizumi, *Improving fuel economy with modtc without increasing TEOST33C deposit*, in *Society of Tribologists and Lubrication Engineers Annual Meeting and Exhibition 2015*. 2015: Dallas, TX, USA. p. 169-171.
24. Khaemba, D.N., A. Neville, and A. Morina, *New insights on the decomposition mechanism of Molybdenum DialkyldiThioCarbamate (MoDTC): a Raman spectroscopic study.* RSC Adv., 2016. **6**(45): p. 38637-38646. DOI: 10.1039/C6RA00652C.
25. Chang, C.H. and S.S. Chan, *Infrared and Raman studies of amorphous MoS_3 and poorly crystalline MoS_2.* Journal of Catalysis, 1981. **72**(1): p. 139-148. DOI: 10.1016/0021-9517(81)90085-3.
26. Weber, T., J.C. Muijsers, and J.W. Niemantsverdriet, *Structure of Amorphous MoS_3.* The Journal of Physical Chemistry, 1995. **99**(22): p. 9194-9200. DOI: 10.1021/j100022a037.

27. Rai, Y., A. Neville, and A. Morina, *Transient processes of MoS_2 tribofilm formation under boundary lubrication.* Lubr. Sci., 2016. **28**(7): p. 449-471. DOI: 10.1002/ls.1342.

28. Windom, B.C., W.G. Sawyer, and D.W. Hahn, *A Raman Spectroscopic Study of MoS_2 and MoO_3: Applications to Tribological Systems.* Tribol. Lett., 2011. **42**(3): p. 301-310. DOI: 10.1007/s11249-011-9774-x.

29. Dobrenizki, L., et al., *Efficiency improvement in automobile bucket tappet/camshaft contacts by DLC coatings – Influence of engine oil, temperature and camshaft speed.* Surf. Coat. Technol., 2016. **308**: p. 360-373. DOI: 10.1016/j.surfcoat.2016.09.041.

30. Kushwaha, M. and H. Rahnejat, *Transient elastohydrodynamic lubrication of finite line conjunction of cam to follower concentrated contact.* J. Phys. D Appl. Phys., 2002. **35**(21): p. 2872. DOI: 10.1088/0022-3727/35/21/327.

31. Ofune, M., et al., *Development of valve train rig for assessment of cam/follower tribochemistry.* Tribol. Int., 2016. **93, Part B**: p. 733-744. DOI: 10.1016/j.triboint.2015.02.026.

32. Al-Jeboori, Y., et al., *The effect of clearance between tappet insert and camlobe on the tribological and tribochemical performance of cam/follower surfaces.* Tribol. Int., 2018. DOI: 10.1016/j.triboint.2018.09.021.

33. Kano, M., Y. Yasuda, and J.P. Ye, *The effect of ZDDP and MoDTC additives in engine oil on the friction properties of DLC-coated and steel cam followers.* Lubr. Sci., 2004. **17**(1): p. 95-103. DOI: 10.1002/ls.3010170108.

34. Sugimoto, I., F. Honda, and K. Inoue, *Analysis of wear behavior and graphitization of hydrogenated DLC under boundary lubricant with MoDTC.* Wear, 2013. **305**(1–2): p. 124-128. DOI: 10.1016/j.wear.2013.04.030.

35. Mufti, R.A., et al., *Innovative technique of measuring follower rotation in real production engine using Gradiometer sensor and the effect of friction modifier.* Ind. Lubr. Tribol., 2015. **67**(4): p. 285-291. DOI: 10.1108/ILT-07-2013-0076.

36. Al-Jeboori, Y., et al., *Measuring tappet rotation in a valvetrain rig when lubricated in a fully formulated oil containing MoDTC-type friction modifier.* Tribol. Int., 2018. **121**: p. 442-449. DOI: 10.1016/j.triboint.2018.01.061.

37. Mufti, R.A. and A. Jefferies, *Novel method of measuring tappet rotation and the effect of lubricant rheology.* Tribol. Int., 2008. **41**(11): p. 1039-1048. DOI: 10.1016/j.triboint.2008.02.016.

38. Morina, A., et al., *ZDDP and MoDTC interactions and their effect on tribological performance – tribofilm characteristics and its evolution.* Tribol. Lett., 2006. **24**(3): p. 243-256. DOI: 10.1007/s11249-006-9123-7.

39. Uy, D., et al., *Characterization of gasoline soot and comparison to diesel soot: Morphology, chemistry, and wear.* Tribol. Int., 2014. **80**: p. 198-209. DOI: 10.1016/j.triboint.2014.06.009.

40. Uy, D., et al., *Characterization of anti-wear films formed from fresh and aged engine oils.* Wear, 2007. **263**(7–12): p. 1165-1174. DOI: 10.1016/j.wear.2006.12.026.

41. de Feo, M., et al., *MoDTC lubrication of DLC-involving contacts. Impact of MoDTC degradation.* Wear, 2016. **348–349**: p. 116-125. DOI: 10.1016/j.wear.2015.12.001.

42. Kosarieh, S., et al., *Wear Mechanisms of Hydrogenated DLC in Oils Containing MoDTC.* Tribol. Lett., 2016. **64**(1): p. 4. DOI: 10.1007/s11249-016-0737-0.

43. Jiménez, A.E., et al., *Surface interactions and tribochemistry in boundary lubrication of hypereutectic aluminium—silicon alloys.* Proc. Inst. Mech. Eng. Part J J. Eng. Tribol., 2009. **223**(3): p. 593-601. DOI: 10.1243/13506501jet528.

44. de Faria, D.L.A., S. Venâncio Silva, and M.T. de Oliveira, *Raman microspectroscopy of some iron oxides and oxyhydroxides.* J. Raman Spectrosc., 1997. **28**(11): p. 873-878. DOI: 10.1002/(SICI)1097-4555(199711)28:11<873::AID-JRS177>3.0.CO;2-B.

45. Repka, M., et al., *Lubricant-surface interactions of polymer-coated engine journal bearings.* Tribol. Int., 2017. **109**: p. 519-528. DOI: 10.1016/j.triboint.2017.01.017.

46. Taylor, O.P., et al., *Tribological Behavior of Low Viscosity Lubricants in the Piston to Bore Zone of a Modern Spark Ignition Engine*, in *SAE 2014 International Powertrain, Fuels & Lubricants Meeting*. 2014, SAE Technical Paper 2014-01-2859: Birmingham, UK. DOI: 10.4271/2014-01-2859.

47. Wichtl, R., et al., *Experimental and Simulative Friction Analysis of a Fired Passenger Car Diesel Engine with Focus on the Cranktrain.* SAE International Journal of Engines, 2016. **9**(4): p. 2227-2241. DOI: 10.4271/2016-01-2348.